Available online at www.sciencedirect.com
SCIENCE DIRECT®
Pergamon
Cement and Concrete Research 33 (2003) 1925–1932
CEMENT AND CONCRETE RESEARCH

Measuring permeability and stress relaxation of young cement paste by beam bending

W. Vichit-Vadakan[1], George W. Scherer*

Department of Civil and Environmental Engineering, Princeton University, Engineering Quad, E-319, CEE/PMI Princeton, NJ 08544, USA

Received 10 April 2003; accepted 22 April 2003

Abstract

When a saturated rod of a porous material is deflected in three-point bending, two types of time-dependent relaxation processes occur simultaneously: hydrodynamic relaxation, caused by the flow of liquid in the porous body, and viscoelastic (VE) relaxation of the solid network. By measuring the decrease in the force required to sustain a constant deflection, it is possible to obtain the permeability from the hydrodynamic relaxation function, in addition to the VE stress relaxation function of the sample. We report the early-age evolution of permeability, elastic modulus, and stress relaxation function for Type III Portland cement paste with water–cement (w/c) ratios of 0.45, 0.50, and 0.55. The stress relaxation function is shown to preserve its shape during aging; that function is numerically transformed into the creep function.

Keywords: Cement paste; Creep; Elastic moduli; Permeability; Stress relaxation

1. Introduction

The permeability of cement paste, mortars, and concrete is difficult to measure reproducibly and accurately with conventional techniques due to the amount of time required and the risk of leaks at high pressure. The beam-bending method previously introduced [1] and verified [2] is a novel way to make such measurements. When a saturated elastic porous body is suddenly deflected under three-point bending, a pressure gradient develops in the pore liquid. As the gradient is relieved by flow through the pores, the load required to maintain a fixed deflection also decreases and plateaus as ambient pressure is restored in the pore liquid. The permeability of the body can be found by analyzing the rate of load relaxation. In a viscoelastic (VE) body, such as cement paste, the load continues to decrease as the solid phase in the porous body relaxes viscoelastically. Thus, in addition to yielding the permeability, the bending method also yields the elastic modulus and stress relaxation function of the material. The measurement and analysis together typically take a few minutes to a few hours to complete. The purpose of this study is to quantify the basic creep behavior of cement paste. The functional form of the stress relaxation function is established by the beam-bending experiments, and the stress relaxation function is transformed into the creep function using numerical methods.

When a linearly elastic cylindrical sample is subjected to a constant deflection in three-point bending, the hydrodynamic relaxation function, $R(t)$, is

$$R(t) = \frac{W(t)}{W(0)} = 1 - A + A\sum_{n=1}^{\infty} \frac{8}{\beta_n^2} \exp \frac{-\beta_n^2 t}{\tau_R} \tag{1}$$

where $W(t)$ is the force measured at time t, β_n are roots of the Bessel functions $J_1(B_n) = 0$, and the constant A is given by

$$A = \frac{\left(\frac{1-2\nu_p}{3}\right)\left(1-\frac{K_p}{K_S}\right)^2}{1-\frac{K_p}{K_S}+(1-\rho)\left(\frac{K_p}{K_L}-\frac{K_p}{K_S}\right)} \tag{2}$$

The hydrodynamic relaxation time, τ_R, is defined by

$$\tau_R = \frac{\mu_b(1-2\nu_p)R^2\eta_L}{G_p D} \tag{3}$$

* Corresponding author. Tel.: +1-609-258-5680; fax: +1-609-258-1563.
E-mail address: scherer@princeton.edu (G.W. Scherer).
[1] Present address: Department of Civil Engineering and Geological Sciences, University of Notre Dame, 160 Fitzpatrick Hall, Notre Dame, IN 46556, USA.

0008-8846/$ – see front matter © 2003 Elsevier Ltd. All rights reserved.
doi:10.1016/S0008-8846(03)00168-6

and

$$\mu_b = \left(1 - \frac{K_p}{K_S}\right) + \frac{(1-\rho)G_p}{(1-2\nu_p)K_L} + \frac{(\rho - K_p/K_S)G_p}{(1-2\nu_p)K_S} \quad (4)$$

where R is the radius of the sample, η_L is the viscosity of the pore liquid, D is the permeability of the porous body, ρ is the volume fraction of solids in the porous body, ν is Poisson's ratio, K is the bulk modulus, G is the shear modulus, and subscripts, p, S, and L represent the properties of the drained porous body, solid phase, and liquid phase, respectively. Young's modulus can be extracted from the initial load W_0, A, and geometric parameters by

$$E_p = \frac{W_0(1-A)L^3}{48I\Delta} \quad (5)$$

where L is the support span, I is the moment of inertia of the sample ($=\pi R^4/4$ for a cylinder), and Δ is the applied displacement. Evaluation of the rigorous solution for the relaxation of a VE porous body shows that the relaxation behavior can be approximated, to a very high degree of accuracy, by the product of the hydrodynamic relaxation function, given by Eq. (1), and the VE relaxation function, $\psi_{VE}(t)$, as follows [1]

$$\frac{W(t)}{W(0)} = R(t)\psi_{VE}(t) \quad (6)$$

In this case, Eq. (5) represents the instantaneous elastic modulus of the drained network.

A wide variety of VE relaxation processes have been shown to fit the stretched exponential (SE) function [3],

$$\psi_{VE}(t) = \exp\left[-\left(\frac{t}{\tau_{VE}}\right)^b\right] \quad (7)$$

This function is very convenient for fitting data because it involves only two fitting parameters. However, it will be demonstrated that this simple function cannot describe the short- and long-term behavior of cement paste. A modification of this function will be introduced and shown to fit the stress relaxation data well. The stress relaxation function will be numerically transformed into the creep function and shown to yield the power law that is observed experimentally.

2. Method

Cement paste with water–cement ratios (w/c) of 0.45, 0.50, and 0.55 were prepared by hand-mixing deionized water and Type III Portland cement with a spatula in a plastic bowl for 100 strokes. Then, the bowl and its contents were placed in a vacuum desiccator for 2 min under house vacuum followed by hand mixing for 50 strokes. The mixing process, followed by a period in the vacuum desiccator, was repeated twice. The samples were cast in 10-ml polystyrene pipettes prelubricated with a thin later of petroleum jelly. The paste was pushed into the pipette with an icing bag. The samples were left to cure standing on end for 18 h and demolded by pushing out the sample with a metal rod of a similar diameter. The petroleum jelly was manually removed from the surface of the sample with paper towels. The ends of the samples were trimmed on a diamond saw and the rods were labeled and placed in a lime-saturated bath for curing at room temperature until the time of testing.

The beam-bending apparatus was described previously [2]. Briefly, a stepper motor controls the movement of a load cell (±250 g range) attached to a push rod that goes through an LVDT (0–10 mm range). This system is set in a frame attached to a bath that allows the sample to sit on supports spanning up to 280 mm while the sample is immersed in lime water; all components were made out of stainless steel. The data were logged with a 16-bit A/D converter controlled by Dasylab 5.0 software. Typical experimental parameters include sample diameter of 7.7 mm, span of 250 mm, and deflection of 100–150 μm. These parameters yielded applied strains of $\sim 8 \times 10^{-5}$ and stresses on the order of 1 MPa. The theory relies on the sample being fully saturated, and it has been shown that these samples are thin enough to maintain full saturation when cured under atmospheric pressure in a lime water bath [4].

The load relaxation data were fitted to Eqs. (1), (6), and (7) with the Nelder–Mead algorithm [5], with $R(t)$ given by Eq. (1) [1]. Fig. 1 shows a typical fitted data set, along with the hydrodynamic and VE relaxation functions. In particular, this data set is for a 3-day-old sample with w/c = 0.55.

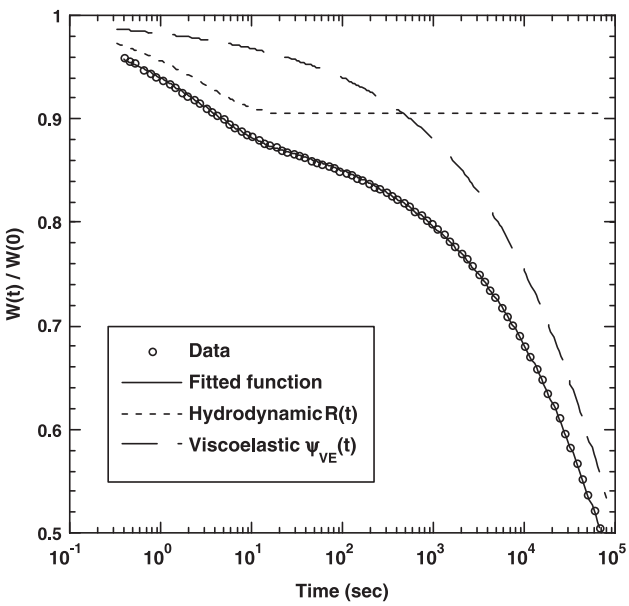

Fig. 1. Typical fit to relaxation curve with the hydrodynamic and VE relaxation functions. Data set from sample that is 3 days old (w/c = 0.55).

3. Results and discussion

3.1. Stress relaxation

Fig. 2 shows a series of relaxation curves for w/c = 0.45 at various ages. The inflection in the relaxation curve corresponds to the end of the hydrodynamic relaxation; subsequent relaxation is VE. The shift of the inflection points to longer times indicates a decrease in the permeability with age. Table 1 shows the evolution of the permeability and mechanical properties at various w/c and ages. The VE relaxation functions extracted from the data are plotted in Fig. 3, which clearly shows that the rate of stress relaxation decreases as the sample ages.

The validity of Eq. (1) has been demonstrated for porous elastic solids [2]; moreover, Eqs. (6) and (7) have proven to be accurate for silica gels [6]. In contrast, for cement paste, we find that the VE relaxation function is not accurately fitted by an SE function when the stress relaxes more than 15–20%. The SE function can be linearized by plotting $\ln[-\ln(\psi_{VE})]$ against $\ln(t)$; the resulting slope is b and the intercept is $-b\ln\tau_{VE}$. Fig. 4 shows the linearized plot of the VE relaxation function for a 1.5-day-old sample with w/c = 0.50. Instead of a single straight line, there is a bend in the curve when $\ln(t) \approx 7$ leading to a second linear region; each such region can be represented by an SE function with a different exponent, b, and characteristic time, τ_{VE}. The stress relaxation function shows this behavior in all of our cement pastes.

These results imply that one SE function applies at early times and another applies later. If the relaxation function resembles a function, $f_1(t)$, when ψ_{VE} approaches 1, and resembles a second function, $f_2(t)$, when ψ_{VE} approaches 0, then

$$\psi_{VE} \approx \psi_{VE} \cdot f_1(t) + (1 - \psi_{VE}) \cdot f_2(t) \tag{8}$$

The solution of Eq. (8) is

$$\psi_{VE} = \frac{f_2(t)}{1 - f_1(t) + f_2(t)} \tag{9}$$

Since Fig. 4 shows linearity in two sections, $f_1(t)$ and $f_2(t)$ are both SE functions. The relaxation function is therefore

$$\psi_{VE}(t) = \frac{\exp\left[-\left(\frac{t}{\tau_2}\right)^{b_2}\right]}{1 - \exp\left[-\left(\frac{t}{\tau_1}\right)^{b_1}\right] + \exp\left[-\left(\frac{t}{\tau_2}\right)^{b_2}\right]} \tag{10}$$

The additional two fitting parameters can be accurately determined by fitting, because the curve, when plotted in the

Table 1
Permeability and Young's modulus

Age (days)	w/c = 0.45		w/c = 0.50		w/c = 0.55	
	E_p (GPa)	D (nm^2)	E_p (GPa)	D (nm^2)	E_p (GPa)	D (nm^2)
1	11.1	0.177	10.8	0.121		
1.5	11.5	0.0328	11.8	0.0246		
2	14.5	0.00456	12.4	0.00653	10.6	0.580
2.5	13.6	0.000928	13.5	0.000431	10.6	1.42
3	15.6	0.000593			11.2	0.0937
4			12.7	0.000193	10.7	0.115

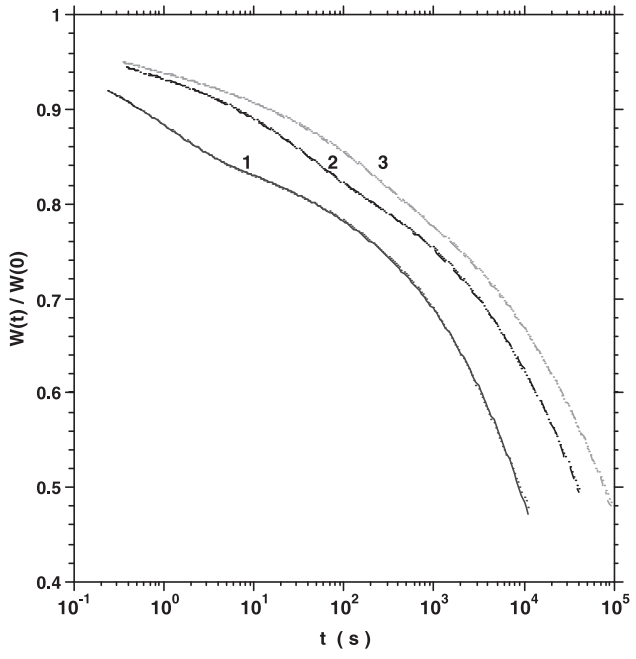

Fig. 2. Load relaxation curves for paste with w/c = 0.45, aged 1, 2, or 3 days before start of measurement; age is indicated by number on curve. Data are symbols and curves are fits of data to Eqs. (1), (6), and (10).

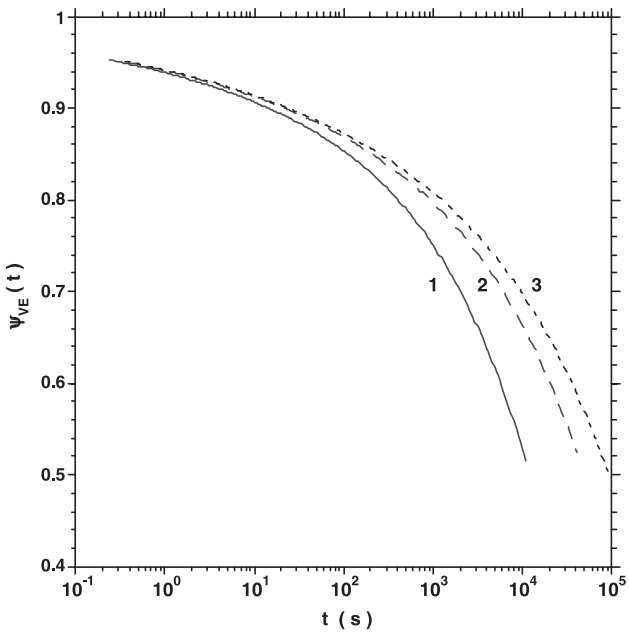

Fig. 3. Stress relaxation function for paste with w/c = 0.45, aged 1, 2, or 3 days before start of measurement; age is indicated by number on curve.

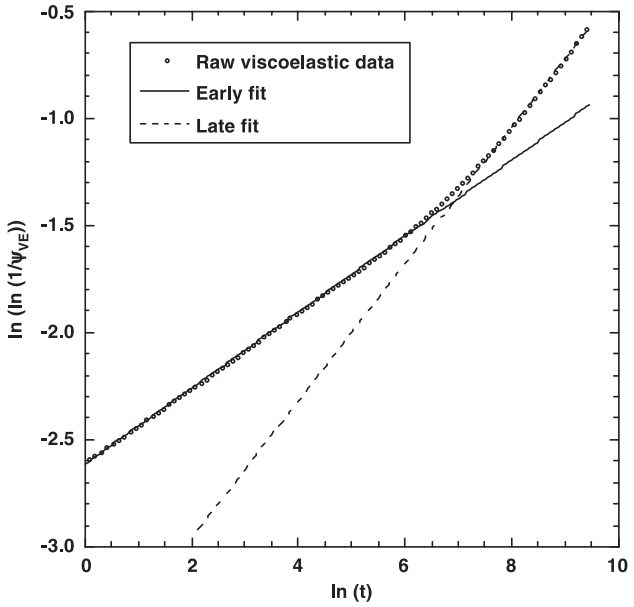

Fig. 4. Linearized plot of measured stress relaxation function (symbols) showing two different linear regions, at early and late times. Data for paste with w/c = 0.50 aged 1.5 days before start of measurement.

linearized form as shown in Fig. 4, displays two distinct linear regions.

We find that we can fit all of our data for stress relaxation in samples ranging in age from 1 to 4 days and w/c from 0.45 to 0.55 using the same two exponents in Eq. (10): $b_1 = 0.18$ and $b_2 = 0.35$. The quality of the fits for the samples with w/c = 0.45 is shown in Fig. 2. Fig. 5 shows

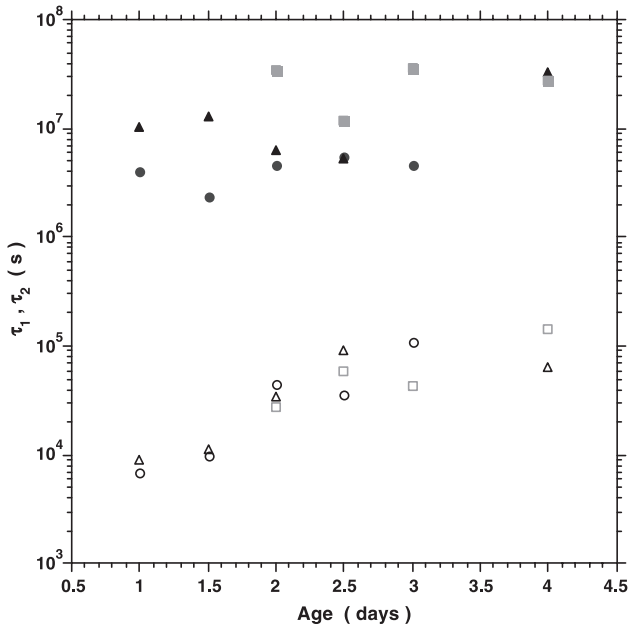

Fig. 5. Relaxation times obtained from fit of Eq. (10) to relaxation data with $b_1 = 0.18$ and $b_2 = 0.35$; solid symbols are τ_1 and open symbols are τ_2 for w/c ratios of 0.45 (●,○), 0.50 (▲,△), and 0.55 (■,□).

that the relaxation times τ_1 and τ_2 differ by about two orders of magnitude; τ_1 shows no obvious trend with age, but τ_2 increases.

The average VE relaxation time is [3]

$$\bar{\tau}_{VE} = \int_0^\infty \psi_{VE}(t)\mathrm{d}t = \frac{3\eta_p}{E_p} \tag{11}$$

where η_p is the viscosity of the paste and E_p is Young's modulus. Eq. (10) cannot be integrated analytically, so numerical integration is used to calculate the average VE relaxation time; the results are shown in Table 2. Fig. 6 shows that the viscosity rises by about an order of magnitude over 3 days of aging. It is the progressive increase in $\bar{\tau}_{VE}$ (or η_p) that causes the curves in Fig. 3 to shift further to the right with age.

A function, such as that in Eq. (10), that decreases monotonically can be approximated by a finite sum of N exponential terms [3]:

$$\psi_{VE}(t) = \sum_{k=1}^{N} w_k \exp(-t/\tau_k) \tag{12}$$

where the weighting coefficients sum to unity, $\sum_{k=1}^{N} w_k = 1$, and the relaxation times, τ_k, span several orders of magnitude. An efficient algorithm for performing such fits was developed previously [7]. Fig. 7 shows a sample fit of Eq. (12) to Eq. (10) using 30 terms; also shown are the SE functions, $f_1(t)$ and $f_2(t)$. The distribution of relaxation times is shown in Fig. 8a for samples aged 1–3 days. The curves shift to longer times in the older samples, but when the relaxation times are normalized by the respective value of $\bar{\tau}_{VE}$ for each sample, as in Fig. 8b, the distributions are seen to be virtually identical.

Since the exponents b_1 and b_2 remain constant while the relaxation times increase, the aging that occurs during the

Table 2
Stress relaxation fitting parameters

w/c	Age	τ_1 (10^6 s)	τ_2 (10^3 s)	$\bar{\tau}_{VE}$(10^5 s)	η_p (10^{14} Pa s)
0.45	1	4.1	7.0	0.67	2.5
	1.5	2.4	9.7	0.84	3.2
	2	4.7	45.5	3.63	17.5
	2.5	5.5	36.0	2.99	13.6
	3	4.7	111.0	8.12	42.1
0.50	1	10.5	8.9	0.91	3.3
	1.5	13.0	11.5	1.17	4.6
	2	6.4	34.0	2.88	11.9
	2.5	5.3	91.3	6.89	31.0
	4	32.5	65.5	6.13	26.0
0.55	2	34.5	27.8	2.88	10.2
	2.5	12.0	59.5	5.08	18.0
	3	36.4	43.2	4.28	15.9
	4	27.0	141.0	12.0	42.7

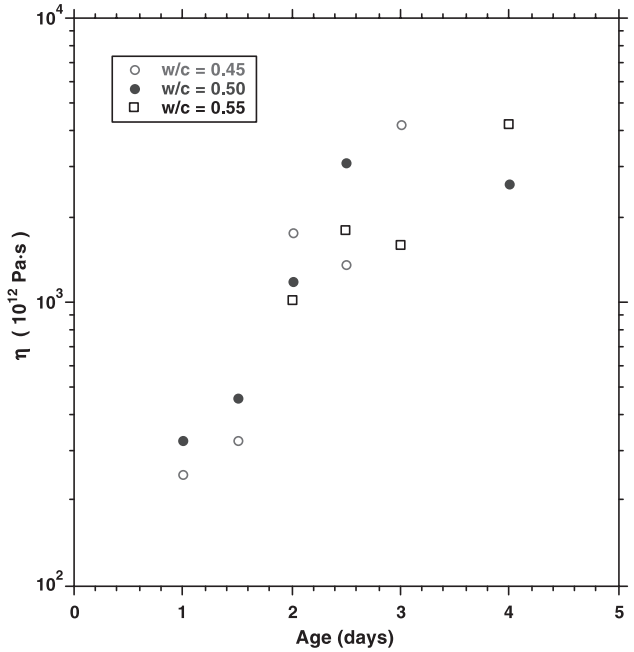

Fig. 6. Evolution of the viscosity of the porous body with age for pastes with w/c = 0.45, 0.50, and 0.55.

experiment can be taken into account by writing each SE function as

$$f_k = \exp\left[-\left(\int_0^t \frac{dt'}{\tau_k}\right)^{b_k}\right] \quad \text{where } k = 1, 2 \tag{13}$$

In the present experiments, the duration of the test was short enough, compared to the age of the sample, that only a modest change in degree of hydration would be expected to occur during the measurement. For a paste that was 1 day old at the start of the run, the time required to achieve 50% relaxation of the stress was 4 h; the same degree of relaxation was obtained in 12, 24, and 48 h for samples aged 2, 3, and 4 days, respectively. Owing to the short duration of the experiments, we expect that the relaxation times were nearly constant during the measurement.

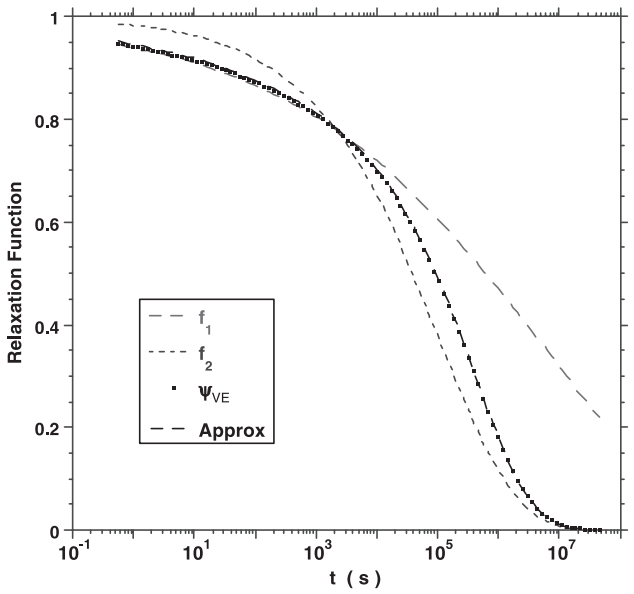

Fig. 7. Measured stress relaxation function (symbols) fit to Eq. (12) (Approx), together with the two SE functions, $f_1(t)$ and $f_2(t)$.

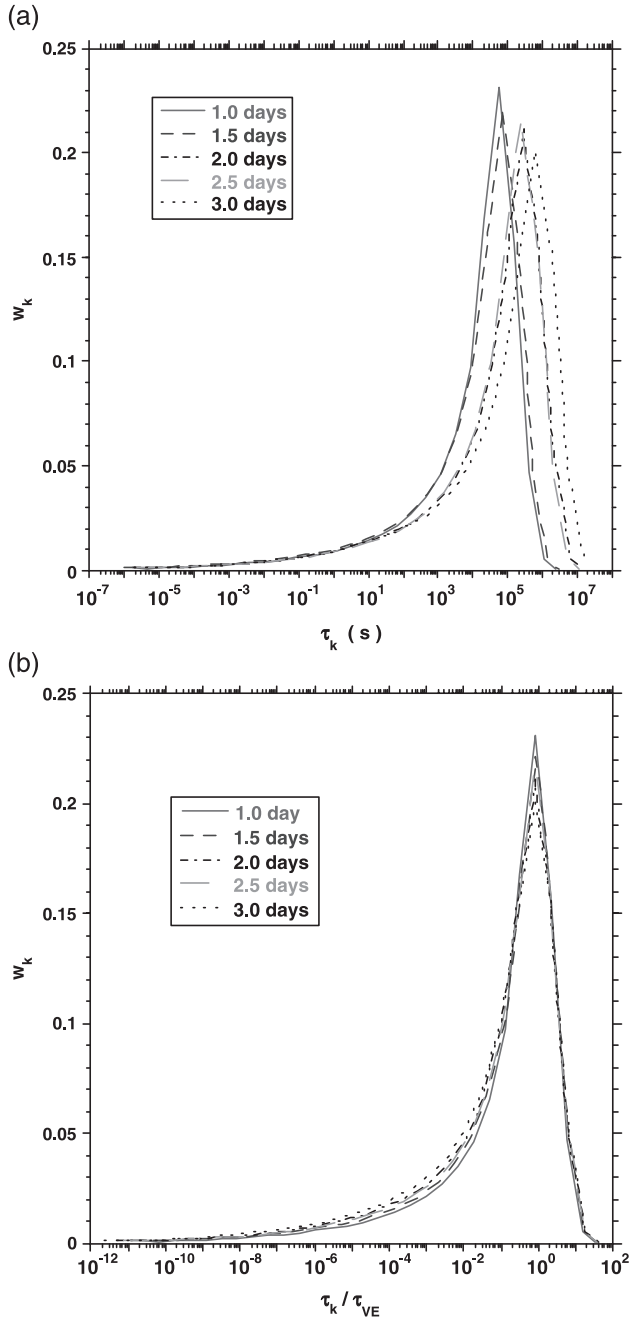

Fig. 8. (a) Distribution of relaxation times obtained by fitting Eqs. (10)–(12), for paste with w/c = 0.45 aged 1–3 days before start of measurement. (b) Same curves as in (a), but the relaxation times are normalized by the average relaxation time for each sample.

Bazant and Ferretti [8] attribute aging of young samples to the change in the degree of hydration of the paste. The chemical reaction eliminates unhydrated cement, which acts as reinforcement, and produces more calcium–silicate–hydrate (C-S-H), which is the phase responsible for VE deformation. Unfortunately, in the present study, we neglected to measure the degree of hydration, but that will be done in future work. By performing a series of relatively short relaxation experiments, we will be able to quantify the change in τ_1 and τ_2 with degree of hydration; then it should be possible to predict the course of longer relaxation experiments.

Older samples also show a decreasing creep rate, although little hydration is occurring; this is attributed by Bazant and Ferretti [8] to spontaneous relaxation of the micro-prestressed regions. It seems likely that those regions would relax even more rapidly in young samples, where the molecular mobility is greater, so restructuring of the C-S-H is probably an important cause of aging in both young and old samples.

3.2. Creep

The uniaxial compliance function, $J(t)$, is given by [3]

$$J(t) \equiv \frac{\phi(t)}{E_0} = \frac{1}{E_\infty} - \left(\frac{1}{E_\infty} - \frac{1}{E_0}\right)\phi_d(t) + \frac{t}{3\eta} \tag{14}$$

where $\phi(t)$ is the creep function, E_0 is the instantaneous elastic modulus, E_∞ is the infinite-time elastic modulus, $\phi_d(t)$ is the delayed elastic retardation function, and η is the viscosity; for a porous material, E_0 corresponds to E_p and η corresponds to η_p appearing in Eq. (11). In writing Eq. (14), it is assumed that the viscosity and relaxation times are constant; when that condition does not apply, the creep function takes the form given below in Eq. (23). When $t=0$ (i.e., immediately after a constant stress is applied), $J(0)=1/E_0$; as time increases, $\phi_d(t)$ relaxes from 1 toward 0, so the elastic compliance increases from $1/E_0$ to $1/E_\infty$. The creep and stress relaxation functions are related by [3]

$$t = \int_0^t \psi_{VE}(t-t')\phi(t')\mathrm{d}t' \tag{15}$$

Since the stress relaxation function is known to have the form given in Eq. (10), $\phi(t)$ can be calculated by applying the Laplace transform to Eq. (15). The transform of a function $f(t)$ with respect to time is defined by [9]

$$\hat{f}(s) = \int_0^\infty \mathrm{e}^{-st} f(t)\mathrm{d}t \tag{16}$$

where $\hat{f}$ indicates the Laplace transform of the function f and s is the transform parameter. The transform of Eq. (15) leads to

$$\hat{\phi} = \frac{1}{s^2\hat{\psi}_{VE}} \tag{17}$$

When ψ_{VE} is represented by a sum of exponential terms, as in Eq. (12), then the Laplace transform is the quotient of two polynomials in s. In that case, the right side of Eq. (17) can be separated into partial fractions [10]; when the transform is inverted, it has the form of Eq. (14) with

$$\phi(t) = \alpha - (\alpha - 1)\sum_{k=1}^{N-1} v_k \exp(-t/\tau_k') + \frac{t}{\bar{\tau}_{VE}} \tag{18}$$

where the v_k are weighting factors that sum to unity, $\sum\sum_{k=1}^{N-1} v_k = 1$, and

$$\alpha = \frac{\sum_{k=1}^{N} w_k \tau_k^2}{\left(\sum_{k=1}^{N} w_k \tau_k\right)^2} = \frac{\int_0^t \psi_{VE}(t)t\ \mathrm{d}t}{\left(\int_0^t \psi_{VE}(t)\mathrm{d}t\right)^2} \tag{19}$$

Comparison to Eq. (11) reveals that the denominator of the right side of Eq. (19) is $\bar{\tau}_{VE}{}^2$. Comparing Eqs. (14) and (18), we see that

$$\alpha = \frac{E_0}{E_\infty} \tag{20}$$

so the magnitude of the delayed elastic strain is related to the distribution of relaxation times. Thus, all of the factors in the creep equation can be determined if the stress relaxation function is known. In particular, we can predict the delayed elastic strain and the viscosity of cement paste from our data for ψ_{VE}.

The preceding analysis is valid even when aging occurs during the measurement, on the following condition. If the relaxation times all change at the same rate during aging, then they can be written as constant multiples of some particular relaxation time, such as $\bar{\tau}_{VE}$:

$$\tau_k = \bar{\tau}_{VE}/\lambda_k \tag{21}$$

where the λ_k are constants. Then we can define a dimensionless time,

$$\xi = \int_0^t \frac{\mathrm{d}t'}{\bar{\tau}_{VE}} \tag{22}$$

and the creep function becomes

$$\phi(\xi) = \alpha - (\alpha - 1)\sum_{k=1}^{N-1} v_k \exp(-\lambda_k \xi) + \xi \tag{23}$$

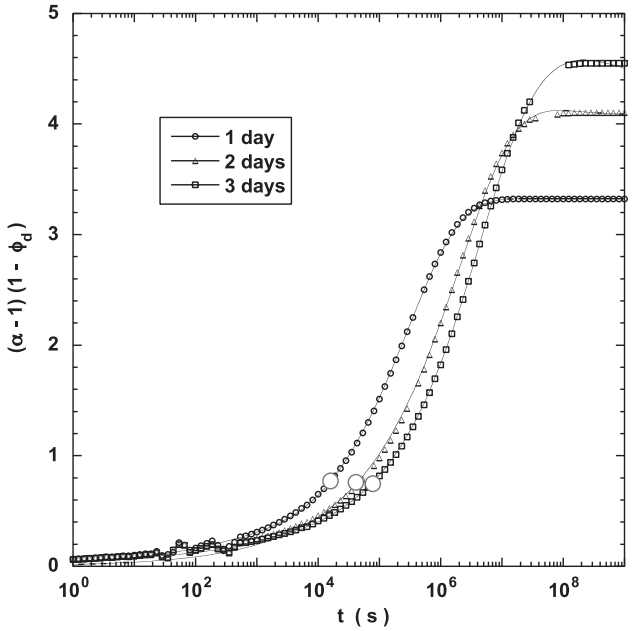

Fig. 9. Delayed elastic retardation function, $\phi_d(t)$, obtained by numerical inversion of Eq. (17) for paste with w/c = 0.45; large circle indicates time at which beam-bending measurement ended.

In this case, Eq. (17) still applies, except that the Laplace transform must be applied with respect to ξ, rather than t. Analogous behavior is seen in the relaxation of stress in glass: following a change in temperature, the structure of glass approaches equilibrium slowly and the viscosity changes continuously toward equilibrium; the kinetics of stress relaxation are accurately predicted by assuming that each relaxation time in the distribution changes in parallel with the viscosity [3,14]. For Eq. (21) to be an acceptable approximation for cement paste, the relaxation times τ_1 and τ_2 must change at the same rate; the data in Fig. 5 are not conclusive on this point, so further experimentation is required.

It is difficult to offer a physical justification for the validity of Eq. (21) for glass or cement, since the physical origin of the relaxation times is not understood. However, one might argue that the young paste contains tenuous links consisting of highly strained bonds that break and reform, or are reinforced by additional hydration, so that relaxation becomes increasingly difficult. The nonexponential shape of the relaxation function reflects the cooperative process of bond breaking and load transfer, and that process can be slowed without changing qualitatively as the structure matures; therefore, the relaxation function may preserve its shape as aging shifts it to longer times. The strained bonds may be the micro-prestress regions invoked by Bazant and Ferretti [8]. However, they argued [15] that the relaxation behavior must change by addition of newly formed C-S-H and that it violates the principles of thermodynamics for the properties of the material to change such that the relaxation times increase. We argue that the paste is not at equilibrium (so that it is in a condition analogous to that of glass following a rapid change in temperature, where its properties change isothermally as the structure slowly approaches equilibrium [3]), so the bonds are breaking and rearranging in an effort to minimize the energy of the system (and thereby eliminating regions of micro-prestress). The slow approach of the structure to equilibrium should be accompanied by an increase in order that reduces mobility and thereby slows the rate of relaxation.

Due to the complexity of Eq. (10), Eq. (17) cannot be used to obtain an analytical result for ϕ for the cement paste. However, ψ_{VE} can be transformed numerically, then the transform in Eq. (17) can be numerically inverted using the Stehfest function [11]; the calculation is efficiently performed using Mathematica [12].

Fig. 9 shows the delayed elastic retardation function, $(\alpha-1)(1-\phi_d)$, obtained from the stress relaxation function shown in Fig. 2; the scatter near 100 s results from instability in the numerical inversion. The curves shift toward longer times, and the maximum value increases, with the age of the paste; this occurs because aging increases the relaxation times, which control the value of α according to Eq. (19). Fig. 10 shows that a power law function provides a good fit at intermediate values of $\phi_d(t)$, with an exponent of about 0.34; if the fit is applied to the earlier part of the curve, the exponent drops toward 0.2 (converging on the value of b_1). This is consistent with published data for delayed elasticity, which show power-law behavior with an exponent of about 0.25 [13].

It is important to recognize that our stress relaxation experiments were short, so that the sample did not age significantly during the measurement. Consequently, when ψ_{VE} is inverted to obtain the creep function, the result represents the creep that would be observed in a sample at

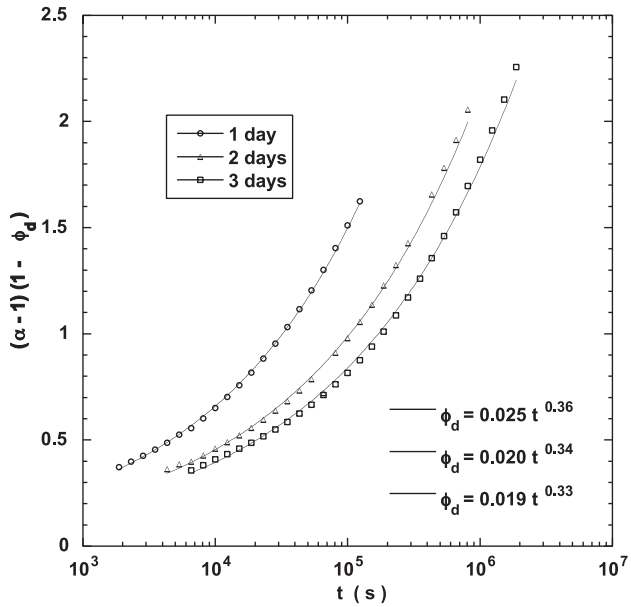

Fig. 10. Power-law fit to delayed elastic retardation functions from Fig. 9 at intermediate times.

a constant degree of hydration. Therefore, the results are not directly comparable to real creep experiments, which have such a long duration that the sample does undergo aging. The present method will be particularly useful for studying the effect of aging on creep, because the stress relaxation experiments provide a ''snapshot'' of the creep behavior in a given state of hydration, so a series of experiments of the kind presented in Fig. 9 make it possible to separate the intrinsic time-dependence of creep from the influence of aging.

4. Conclusions

The stress relaxation function for Type III Portland cement paste has been shown not to fit the simple SE function but the modified function in Eq. (10) offers an excellent fit. The function retains its shape as the sample ages, so the aging process can be represented as a uniform shift in the distribution of relaxation times, analogous to thermorheologically simple behavior. This implies that the effect of aging can be incorporated into the analysis of creep by a simple shift of the time scale. When the relaxation function is numerically inverted to obtain the creep function, the delayed elastic retardation function is found to obey a power law at intermediate times, in agreement with published creep data.

Acknowledgements

W. Vichit-Vadakan was supported by a grant from the Schlumberger Foundation.

References

[1] G.W. Scherer, ''Characterization of Saturated Bodies'', to be published in Concrete Sci. & Eng.[2].
[2] W. Vichit-Vadakan, G.W. Scherer, Measuring permeability of rigid materials by a beam-bending method: II. Porous glass, J. Am. Ceram. Soc. 83 (9) (2000) 2240–2245.
[3] G.W. Scherer, Relaxation of Glass and Composites, Wiley, New York, 1986, pp. 41–43, reprinted by Kreiger, Malabar, FL (1992).
[4] W. Vichit-Vadakan, G.W. Scherer, Measuring permeability of rigid materials by a beam-bending method: III. Cement paste, J. Am. Ceram. Soc. 85 (6) (2002) 1537–1544.
[5] D.M. Olsson, A sequential simplex program for solving minimization problems, J. Qual. Technol. (6) (1974) 53–57.
[6] G.W. Scherer, Relaxation of a viscoelastic gel bar: II. Silica gel, J. Sol–Gel Sci. Technol. 2 (1994) 199–204.
[7] G.W. Scherer, Volume relaxation far from equilibrium, J. Am. Ceram. Soc. 69 (5) (1986) 374–381.
[8] Z.P. Bazant, D. Ferretti, Asymptotic temporal and spatial scaling of coupled creep, aging, diffusion, and fracture processes, in: F.-J. Ulm, Z.P. Bazant, F.H. Wittman (Eds.), Creep, Shrinkage and Durability Mechanics of Concrete and Other Quasi-Brittle Materials, Elsevier, Oxford, UK, 2001, pp. 121–145.
[9] F.B. Hildebrand, Advanced Calculus for Applications, Prentice-Hall, Englewood Cliffs, NJ, 1962, chapter 5.
[10] CRC Standard Mathematical Tables, vol. 13, CRC Press, Boca Raton, FL, 1991.
[11] H. Stehfest, Numerical inversion of Laplace transforms, Commun. ACM 13 (1) (1970) 47–49, 624.
[12] Wolfram Research, Numerical inversion performed using the package NumericalInversion, ©2000 by Arnaud Mallet.
[13] L.P. Granger, Z.P. Bazant, Effect of composition on basic creep of concrete and cement paste, J. Eng. Mech. 121 (1995) 1261–1270.
[14] J. DeBast, P. Gilard, Variation of the viscosity of glass and the relaxation of stresses during stabilization, Phys. Chem. Glasses 4 (4) (1963) 117–128.
[15] Z.P. Bazant, Creep and damage in concrete, in: J. Skalny, S. Mindess (Eds.), Materials Science of Concrete, vol. IV, American Ceramic Society, Westerville, OH, 1995, pp. 355–387.